Available online at www.sciencedirect.com
ScienceDirect
Cement & Concrete Composites 30 (2008) 1–12
Cement & Concrete Composites
www.elsevier.com/locate/cemconcomp

# Modeling rheological behavior of highly flowable mortar using concepts of particle and fluid mechanics

Gang Lu [a], Kejin Wang [a,*], Thomas J. Rudolphi [b]

[a] Iowa State University, 492 Town Engineering, Ames, IA 50011, USA
[b] Iowa State University, 2271 Howe Hall, 2333, Ames, IA 50011, USA

Received 20 November 2006; received in revised form 25 May 2007; accepted 1 June 2007
Available online 30 June 2007

**Abstract**

A particle–fluid model is developed for predicting the relationship between the shear stress and shear strain rate of highly flowable mortars. In this model, mortars are considered as a two-phase material, containing a fluid matrix (cement paste) and a group of well-graded, non-cohesive, and rigid particles (fine aggregate) that are uniformly distributed in the matrix. The mortar shear stress is assumed to be the sum of the shear stresses resulting from the paste flow, the aggregate particle movement, and the interaction between the cement paste and aggregate. The shear stress resulting from the paste flow is assessed using constitutive equations. The shear stress resulting from the aggregate particle movement is evaluated based on the probability and mechanical concepts of aggregate particle collision. The shear stress resulting from the interaction between the paste and aggregate is considered as the normal stress that the moving aggregate particles apply onto the cement paste. The shear rate of the mortar is obtained from the rheological definition of viscosity. Using this model, the effects of mortar mixture properties (such as aggregate size, volume, gradation, and friction as well as paste viscosity and yield stress) on mortar rheology are studied.
Published by Elsevier Ltd.

*Keywords:* Mortar; Model; Rheology; Shear stress

## 1. Introduction

Modern concrete can be designed and produced to have great flowability that allows the concrete mixture to flow into congested reinforcement areas and fill complicated formwork under its own weight without segregation. Such a self-consolidating concrete (SCC) has generated a tremendous industrial interest because of its economic opportunities (reduced labor and accelerated construction), improved concrete quality, and friendly working environment [1]. A great deal of work has been done developing test methods and evaluating the SCC flow properties since the last decade. However, limited research has been conducted studying the mechanism of the concrete flow and self-consolidation. The SCC mix proportioning is now still based on a trial-and-error process. Further development and application of SCC are requiring a better understanding of the fundamental rheological behavior of the concrete materials.

Many models have been developed to study and predict concrete rheological behavior. Among the available models, the Herschel–Bulkley (HB) model is considered as the most suitable for SCC [2,3]. The HB model is expressed as: $\tau = \tau_0' + a \cdot \dot{\gamma}^b$, where $\tau_0'$ is the yield stress, $\dot{\gamma}$ is the shear strain rate, and $a$ and $b$ are concrete material related constants, which commonly result from a curve fitting of available rheology experiment data. As a result, although the HB model is well-accepted by many researchers, it is still a semi-empirical model and the model itself does not directly describe the effects of materials and mix proportion on the concrete rheological behavior.

Topcu and Kocataskin developed a model that relates concrete composition with flow properties based on a

* Corresponding author. Tel.: +1 515294 2152; fax: +1 515 294 8216.
*E-mail address:* kejinw@iastate.edu (K. Wang).

0958-9465/$ - see front matter Published by Elsevier Ltd.
doi:10.1016/j.cemconcomp.2007.06.002

**List of symbols**

$a$, $b$, and $c$ constant factors related to the mortar material properties
$A$ projected area of a sphere aggregate particle
$A_{AVE}$ average cross area of aggregate particles on a horizontal plane in mortar
$A_{particle}$ total surface area of all aggregate particles in the unit volume of mortar
$C_D$ coefficient of the cement paste dragging force
$D$ average diameter of aggregate particles
$D_0$ average diameter of the aggregate particles retained on a given sieve, $i$
$D_i$ average diameter of the $i$th group, $D_i = \frac{(D_i)_{max}+(D_i)_{min}}{2}$
$(D_i)_{max}$ maximum diameter of $i$th group
$(D_i)_{min}$ minimum diameter of $i$th group
$\Delta E$ energy loss due to the two-particle collision
$\Delta E_{collision}$ total energy loss due to particle collision
$\Delta E_{interaction}^{single\ particle}$ energy loss due to interaction between the aggregate particle and cement paste
$\Delta E_{interaction}$ energy loss due to interaction between the aggregate particle and cement paste
$F_{AP}$ force acting on cement paste by a single aggregate particle
$f_i$ volume fraction of the average particles on the $i$th sieve
$k_p$ normal stress coefficient
$m$ average mass of aggregate particles
$N$ number of aggregate particles in a unit plane material
$N_{collision}^{plane}$ number of particles that move from one plane to its adjacent plane
$n_{particle}$ number of aggregate particles in a unit volume of mortar
$P_{collision}^{particle}$ the probability that an aggregate particle may go out of the horizontal plane
$P_C^M(\Phi, \Psi)$ probability of a collision occurring at certain location
$(\Delta P_X)_0$ average momentum change of the two-particle collision in the mean flow direction
$(\Delta P_n)_0$ average momentum change along collision direction
$S$ average distance between the aggregate particles in mortar
$V_A$ volume fraction of aggregate
$V_F$ magnitude of particle fluctuation velocity
$V_P$ total volume of voids in unit volume of mortar
$V_M^n$ relative mean flow velocity between two colliding particles
$(V_M^n)_{AVE}$ average relative mean flow velocity between two colliding particles along $n$ direction
$(V_F^n)_{AVE}$ average relative fluctuation velocity between two colliding particles along $n$ direction
$(V_M^t)_{AVE}$ average relative mean flow velocity between two colliding particles along $t$ direction
$(V_F^t)_{AVE}$ average relative fluctuation velocity between two colliding particles along $t$ direction
$V_{particle}$ volume of single particle
$V_{voids}$ total volume of voids in unit volume of mortar
$v$ aggregate particle velocity
$v_F$ aggregate particle fluctuation velocity
$v_i$ velocity components along $X$ axis
$v_j$ velocity components along $Y$ axis
$v_k$ velocity components along $Z$ axis
$\alpha$ angle of direction, see Fig. 7
$\beta$ angle of direction, see Figs. 7 and 8
$\Phi$ angle of direction, see Fig. 11
$\Psi$ angle of direction, see Fig. 11
$\varepsilon$ coefficient of elastic restitution
$\rho_p$ cement paste density
$\zeta$ energy dissipation, which is always positive definite
$\eta_P$ viscosity of the cement paste in mortar
$\eta_M$ mortar viscosity
$\dot{\gamma}_M$ apparent shear rate of the mortar
$\dot{\gamma}_P$ apparent shear rate of cement paste
$\tau_M$ shear stress of mortar
$\tau_0$ yield stress of the mortar
$\tau_P$ shear stress resulting from the cement paste flow in mortar
$\tau_{FA-P}$ shear stress due to the aggregate–cement paste interaction
$\tau_{FA}$ shear stress generated by the fine aggregate movement
$\mu$ friction coefficient of particles
$\frac{\partial u}{\partial y}$ velocity gradient of mortar

two-phase composite material approach and the law of plastic viscosity [4]. In this model, concrete was considered to consist of two phases: a mortar-matrix phase and a coarse aggregate phase. Using the two-phase material approach, Kurokawa et al. studied the effect of coarse aggregate on concrete rheology [5]. In their study, the yield stress and viscosity of fresh concrete were expressed by the sum of the yield stress and viscosity of matrix mortar and the stress and viscosity resulting from the friction of coarse aggregate, respectively.

Considering fresh concrete as a multiphase material, Pimanmas and Ozawa developed a mathematical model for predicting flow property of fresh concrete based on the energy conservation concept [6]. After carefully studying the shear stress transfer mechanism of fresh concrete, they concluded that the overall shear stress of concrete

would be the sum of the shear stresses generated by each phase and the interaction between different phases. They suggested using a probabilistic method to simulate the collision of aggregate particles. However, their model over-simplified the correlation between aggregate volume fraction and friction as a bi-linear relationship.

In the present study, a model for the flow behavior of a fresh highly-flowable mortar is developed primarily based on theoretical derivations. In this model, the shear stress of a flowing mortar is assessed based on a combination of aggregate particle collision mechanics, particle–fluid mechanics, probability concepts, excess paste theory, and consequential stress transfer mechanism. It is expected that the model development and application will provide researchers and engineers with a fundamental insight into the mechanical and physical behavior of a flowing mortar. Similar to mortar, fresh concrete can also be considered as a composite material consisting of two different phases-a group of large rigid particles (coarse aggregate) dispersed in a fluid matrix (mortar). Therefore, the model developed in the present study for mortar can be easily applied to concrete materials.

## 2. Background and approach

In this study, a fresh mortar is considered as a granular material (fine aggregate) that is well-distributed and suspended in a highly-flowable, viscous fluid (cement paste). Entrapped and entrained air voids in the cement paste are not directly considered. The irregular shaped aggregate particles are simulated as rigid, spherical particles having a gradation similar to the aggregate in the actual mortar.

Since the mortar is highly flowable, excess cement paste is assumed available and it separates aggregate particles. (The excess paste thickness is defined as the average thickness of paste coated on the aggregate particle surfaces divided by the average diameter of the aggregate particles. Researchers have found the excess paste thickness is directly related with the concrete viscosity and yield stress [7–9].) When the mortar begins to flow, the cement paste deforms first due to its low yield stress. Because cement paste is a viscous material, it generates a viscous stress that resists the mortar to flow. In the flowing mortar, aggregate particles, having different sizes, move at different rates, rearrange their positions, and change the distances between themselves (Fig. 1). As a result, shear stresses are generated

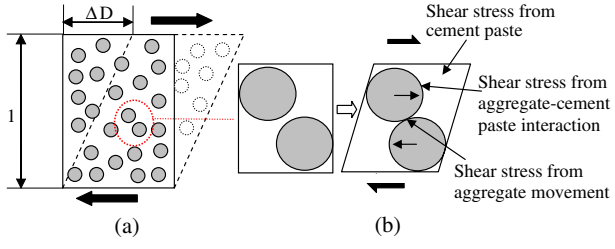


Fig. 1. Material under shear.

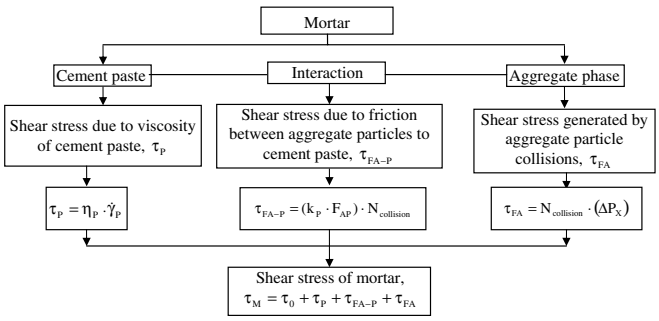


Fig. 2. Modeling approach.

along the flow direction, which is horizontal, in the mortar through the aggregate particle touching, collision, friction, and interlocking. Additional shear stresses are also generated due to the interaction between cement paste and aggregate particles. Therefore, the overall shear stress of a flowing mortar ($\tau_M$) can be taken as the sum of the shear stress resulting from (1) yield stress of cement paste ($\tau_0$), which can be determined from a rheological test or a prediction model; (2) the flow of the cement paste ($\tau_P$), (3) the interaction between the cement paste and aggregate ($\tau_{FA-P}$), and (4) the shear stress resulting from the aggregate movement ($\tau_{FA}$), as expressed by

$$\tau_M = \tau_0 + \tau_P + \tau_{FA-P} + \tau_{FA} \quad (1)$$

In the present study, the shear stress resulting from the cement paste flow ($\tau_P$) is developed based on fluid mechanics concepts. The shear stress resulting from the interaction between the cement paste and aggregate ($\tau_{FA-P}$) is considered to be caused by the friction generated by the normal stress ($F_{AP}$) that the moving aggregate particles apply to the cement paste in front of them, which is equivalent to the resistance applied by the cement paste to the aggregate particle movement. The shear stress resulting from the aggregate movement ($\tau_{FA}$) is evaluated using particle collision mechanics, together with the probability concept. Fig. 2 illustrates the major procedures for the mortar shear stress analysis. The general concepts used for analyzing the shear stress resulting from the aggregate movement ($\tau_{FA}$) are described by: $\tau_{FA} = N_{collision} \cdot (\Delta P_X)_0$, where $N_{collision}$ is the number of colliding particles, and ($\Delta P_X$) is the momentum change per one collision by two particles.

Based on the continuum mechanics, the energy dissipation ($\zeta$) during a solid particle collision is proportional to the shear stress generated by the collision ($\tau_{FA}$), which is in turn proportional to the momentum change of the colliding particles ($\Delta P_X$). Based on the first law of thermodynamics, the energy dissipation ($\zeta$) is also a sum of the energy loss directly due to the particle collision ($\Delta E_{collision}$) and the energy loss due to interaction between the aggregate particle and the cement paste ($\Delta E_{interaction}$):

$$\zeta = \tau_{FA}(\partial u/\partial y) = (N_{collision} \cdot \Delta P_X) \cdot (\partial u/\partial y) \quad (2)$$

$$\zeta = \Delta E_{collision} + \Delta E_{interaction} \quad (3)$$

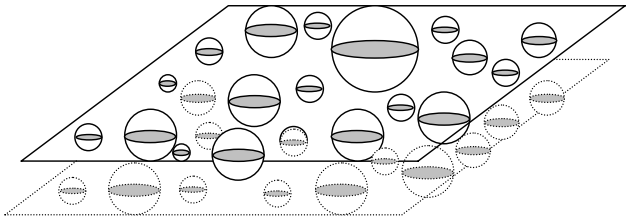

Fig. 3. Aggregate particles on two adjacent planes.

where $\partial u/\partial y$ is the velocity gradient; u is the relative velocity of a flowing material element between two horizontal planes; and $y$ is the vertical distance of this element from the bottom plane.

In the present study, the total momentum change ($\Delta P_X$) is first calculated based on the collision mechanics of a two-particle system. Since aggregate particles in a flowing mortar move without order and unsystematically, the probability concept is applicable. Therefore, the probability of a particle that moves out of its host plane ($P_{\text{collision}}$) and the number of aggregate particles in this host plane are computed. Then, the number of the particles that might move out of their original plane and strike on an adjacent horizontal plane can be determined (Fig. 3). This number is equal to the number of aggregate particle collisions ($N_{\text{collision}}$) that may occur between two adjacent horizontal planes. Thus, the sub-total momentum change ($(\Delta P_X)_p$) due to the aggregate particle collisions in the two adjacent horizontal planes can be calculated by multiplying the momentum change of the two-particle collision system ($(\Delta P_X)_0$) with the number of collisions ($N_{\text{collision}}$) that may occur in the adjacent planes.

Similarly, the energy loss due to the multiple aggregate particle collisions in a mortar unit ($\Delta E_{\text{collision}}$) can also be determined from the number of collisions occurring in the mortar unit. The energy loss due to interaction between aggregate particles and cement paste ($\Delta E_{\text{interaction}}$) can be calculated according to the basic definition of energy: the average dragging force that cement paste applied on the aggregate ($F_{AP}$) multiplied by the average distance between the aggregate particles ($S$). This is because during a collision, one aggregate particle has to move through the inter-particle distance to hit another particle. In this process, the dragging force which the cement paste applied on the moving aggregate particle consumes energy. (The direction of the dragging force is opposite to the aggregate moving direction.)

Combining Eqs. (2) and (3), one can compute the total momentum change ($\Delta P_X$) and finally, calculate the mortar shear stress ($\tau_{FA}$) contributed by the aggregate particle collisions.

## 3. Model development

In the following sections, calculations for each component in the right hand of Eq. (1) are developed. Some assumptions, as listed below, are made to simplify these calculations:

1. All aggregate particles are rigid spherical particles.
2. Cement paste is an ideal viscous flow material.
3. The mortar has a laminar flow, and the shear generated between the mortar layers is in the horizontal direction.
4. Aggregate collisions always occur in the flowing mortar.
5. Flowing aggregate particles have two velocities. One is the mean flow velocity, which is equal to the mean flow velocity of mortar in both magnitude and direction. The other is the fluctuation velocity, which is generated by the particle collisions, and its magnitude is the same for all particles in a given flowing mortar but its direction is random; and
6. There is no static aggregate segregation in mortar.

### 3.1. Yield stress of fresh mortar

Yield stress of a fresh mortar ($\tau_0$) can be determined from a rheological test or a prediction model [10].

### 3.2. Shear stress resulting from cement paste flow ($\tau_P$)

In a flowing mortar, cement paste is primarily a viscous fluid, which provides a viscous stress to resist the flow of the mortar. Therefore, the shear stress of a flowing mortar resulting from its cement paste can be considered as equal to the viscous stress of the cement paste. This viscous stress ($\tau_P$) can be computed from the rheological properties of the cement paste as described in Eq. (4):

$$\tau_P = \eta_P \cdot \dot{\gamma}_P \tag{4}$$

To calculate the shear rate of the cement paste, $\dot{\gamma}_P$, in Eq. (4), a microscopic mortar unit, consisting of two aggregate particles and the cement paste between them (see Fig. 4), is considered. (In Fig. 4, $\gamma_P$ and $\gamma_M$ are shear strain of the cement paste and mortar, respectively; $\dot{\gamma}_P$ and $\dot{\gamma}_M$ are shear rate of the cement paste and mortar, respectively, which are obtained from the shear strain over time ($\Delta T$); $\Delta L$ is the deformation; $h$ is the distance between two particles' gravity centers; $S$ is the distance between two particles' surfaces; and $D$ is the average particle's diameter.) In the microscopic mortar unit system, the shear rate of the aggre-

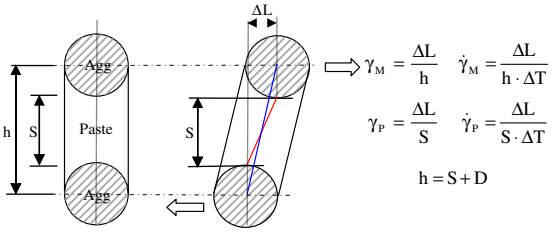


Fig. 4. A microscopic mortar unit under shear.

gate particles is assumed the same as the overall shear rate of the mortar [15]. Thus,

$$\dot{\gamma}_P = \dot{\gamma}_M \cdot \frac{S+D}{S} \tag{5}$$

where $\dot{\gamma}_P$ is the shear rate of cement paste; $\dot{\gamma}_M$ is the shear rate of mortar; and $S$ is the distance between the surfaces of two particles, and as calculated later; $D$ is the average diameter of aggregate particles.

### 3.3. Number of aggregate particle collisions in a flowing mortar ($N_{collision}$)

#### 3.3.1. Modeling aggregate particle distribution

Fig. 5(a) illustrates a unit volume of an actual mortar, which is composed of well-graded, irregular-shaped aggregate particles in a fluid cement paste. The shaded area in plane z represents the aggregate particles and the unshaded area represents the cement paste.

To simplify the collision analysis, these irregular particles are simulated into the sphere particles (Fig. 5(b)) [11]. The various diameters of the spherical aggregate particles can be determined based on the actual aggregate gradation as obtained from the sieve analysis [12], according to Eq. (6) [13]:

$$D_0 = \log^{-1}\left(\frac{\sum_{i=1}^{k} f_i \cdot \log D_i}{\sum f_i}\right) \tag{6}$$

where

$D_0$ is the average diameter of the aggregate particles retained on a given sieve, $i$;
$f_i$ is volume fraction of the aggregate particles on the given sieve;

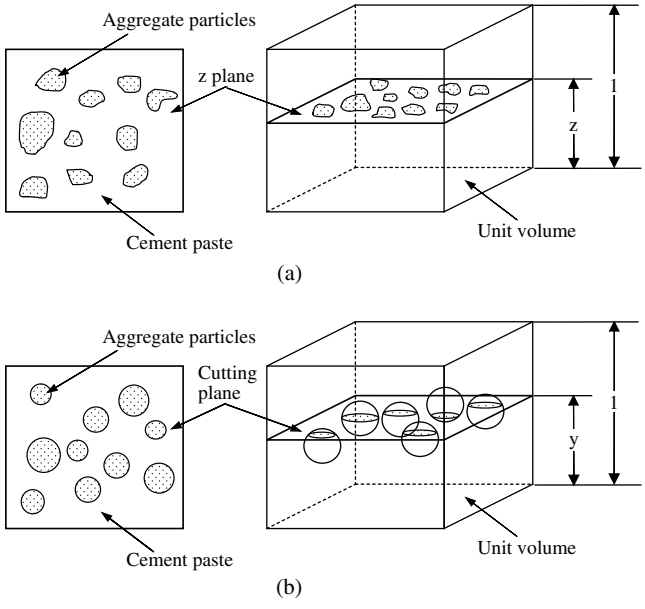


Fig. 5. An aggregate particle intersected by a given horizontal plane before (a) and after (b) simplification.

$D_i$ is the average diameter of the $i$th group, $D_i = \frac{(D_i)_{max}+(D_i)_{min}}{2}$, where $(D_i)_{max}$ is the maximum diameter of $i$th group and
$(D_i)_{min}$ is the minimum diameter of $i$th group; and
$i$ is the order of the sieves used.

Note that plane $y$ intersects aggregate particles with the areas ranging from 0 to $\pi \cdot \left(\frac{D_0}{2}\right)^2$, where $D_0$ is the average diameter of aggregate particles given in Eq. (6).

The average area that a given horizontal plane intersects aggregate particles in the mortar, as shaded area in Fig. 5(b), can be expressed as follows:

$$A_{AVE} = \int_0^{\frac{\pi}{2}} \pi \cdot \left(\frac{D_0}{2}\right)^2 \cdot \cos\alpha \cdot \frac{2}{\pi} \cdot d\alpha = 0.3926 \cdot D_0^2 \tag{7}$$

where $A_{AVE}$ ranges from 0 to $\pi \cdot \left(\frac{D_0}{2}\right)^2$ and $D_0$ is the average diameter of aggregate particles, which can be obtained from Eq. (7).

Assuming that $A_{AVE} = \pi D^2/4$, based on Eq. (7), the average diameter of the aggregate particles intersected by a horizontal plane, $D$, can be calculated as follows:

$$D = 0.7070 \cdot D_0 \tag{8}$$

Note that the aggregate size distribution in any given horizontal plane is considered as the same as that in the entire mortar unit and consistent with the gradation of the aggregate used in the actual mortar. Thus, the total volume of aggregate particles in a unit material element ($1 \times 1 \times 1$) is equal to the volume fraction of aggregate in mortar, $V_A$. The total volume of aggregate particles in a unit material element can be also expressed by the number of aggregate particles in the unit, $N$, multiplies the average volume of the aggregate particles, $A_{AVE}$. Thus,

$$V_A = N \cdot A_{AVE} \tag{9}$$

where

$V_A$ volume fraction of aggregate phase,
$N$ number of aggregate particles in a unit volume material, and
$A_{AVE}$ average area given by Eq. (7).

The number of aggregate particles in a unit material volume was therefore given as

$$N = V_A/A_{AVE} = 1.2732 \cdot \frac{V_A}{D^2} \tag{10}$$

#### 3.3.2. Probability of number of particle collision in a horizontal plane

Based on the discussions above, the irregular arrangement of the aggregate particles in a given horizontal plane (Fig. 6(a)) can be modified into a linear arrangement (Fig. 6(b)). Thus, the probability of a particle "$i$" that may move out of its host horizontal plane and be affected by its adjacent particles can be analyzed. From Fig. 6, the cone surface OPQ is tangent to particle $i$ and its adjacent particles, such as $j$ and $k$. It is assumed that the particle $i$ will not collide with any adjacent particles. Thus, the

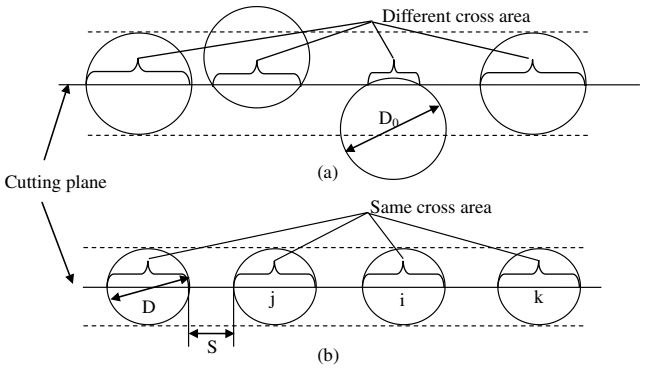


Fig. 6. Particles distribution on one horizontal plane.

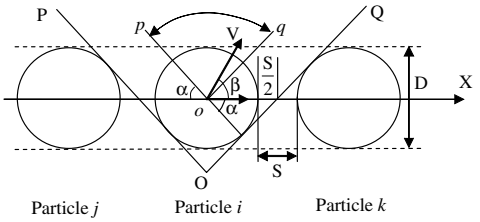


Fig. 7. Direction of velocity of a flowing particle (2-D).

direction of the velocity of the studied particle, $V$, in Fig. 6, should be inside of the cone field *opq* in Fig. 7. The cone OPQ and cone *opq* are parallel to each other.

In the 3-D consideration, the movement of the individual aggregate particle $i$ in Fig. 8 was analyzed as the following:

A typical aggregate particle between two adjacent horizontal planes and intersected by only one of the planes is illustrated as Fig. 8. The angle $\alpha$, which describes the area of the intersection (shaded area), is defined as

$$\sin\alpha = \frac{\frac{D}{2}}{\frac{D}{2}+\frac{S}{2}} = \frac{D}{D+S} \tag{11}$$

where

$D$ average diameter of aggregate particles, given by Eq. (9) and

$S$ average distance between the aggregate particles in mortar.

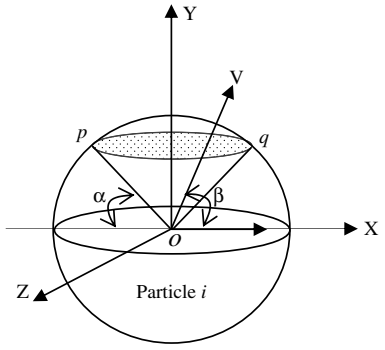


Fig. 8. Individual aggregate particle between two adjacent planes (3-D).

The probability $P_{\text{collision}}^{\text{particle}}$ that an aggregate particle may go out of the horizontal plane (the direction of the particle velocity is within the shaded area in Fig. 8) is the ratio of the surface area of the top segment-to-the surface area of the half sphere:

$$P_{\text{collision}}^{\text{particle}} = \frac{S}{D+S} \tag{12}$$

From Eqs. (10) and (12), the effective number of collisions, $N_{\text{collision}}$ that occurs in this horizontal plane is given by

$$N_{\text{collision}}^{\text{plane}} = N \cdot P_{\text{collision}}^{\text{particle}} = 1.2732 \cdot \frac{V_{\text{A}}}{D^2} \cdot \frac{S}{D+S} \tag{13}$$

Eq. (13) indicates that the effective number of collisions for a unit plane is correlated with the volume fraction of aggregate particles in mortar ($V_{\text{A}}$), their average diameter ($D$), and the distance between the particles ($S$), which is related to the excess paste thickness [8]. When the distance between the aggregate particles ($S$) increases, the effective number of the aggregate collisions ($N_{\text{collision}}^{\text{plane}}$) in a unit plane decreases.

### 3.3.3. Distance between particles in a unit volume of mortar ($S$)

To calculate the distance between the aggregate particles in a unit volume material ($S$), Eq. (14) first gives the volume of a single particle ($V_{\text{particle}}$), and Eq. (15) then provides the number of aggregate particles in a unit volume of the mortar ($n_{\text{particle}}$):

$$V_{\text{particle}} = \frac{4}{3}\pi\left(\frac{D}{2}\right)^3 = \frac{\pi D^3}{6} \tag{14}$$

$$n_{\text{particle}} = V_{\text{A}}/V_{\text{particle}} = \frac{6V_{\text{A}}}{\pi D^3} \tag{15}$$

From Eq. (15), the total surface area of all aggregate particles in the modeled mortar unit ($A_{\text{particle}}$) can be determined from Eq. (16):

$$A_{\text{particle}} = 4\pi\left(\frac{D}{2}\right)^2 \cdot n_{\text{particle}} = \pi D^2 \frac{6V_{\text{A}}}{\pi D^3} = \frac{6V_{\text{A}}}{D} \tag{16}$$

If the mortar aggregate has 35% air voids, in terms of the aggregate volume, after compaction [11] the total volume of voids in the modeled mortar unit will be

$$V_{\text{voids}} = 35\% \times V_{\text{A}} \tag{17}$$

Thus, the average distance between the aggregate particles in the modeled mortar units can be expressed by Eq. (18) [8]:

$$S = 2 \cdot \frac{V_{\text{P}} - V_{\text{voids}}}{A_{\text{particle}}} = \frac{1 - 1.35V_{\text{A}}}{3V_{\text{A}}} \cdot D \tag{18}$$

where $V_{\text{p}}$ is the volume of the cement paste.

Plugging Eqs. (6), (8), and (18) into Eq. (13), one can calculate the number of aggregate particle collision, $N_{\text{collision}}$, in a unit horizontal plane.

### 3.4. Shear stress resulting from the interaction between aggregate and cement paste, $\tau_{FA-P}$

When aggregate particles move faster than the surrounding cement paste in a flowing mortar, they generate a normal force ($F_{\text{AP}}$) on the paste in front of them (Fig. 9). This normal force ($F_{\text{AP}}$) is equal to the drag force

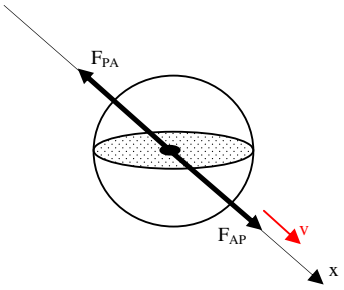


Fig. 9. A spherical particle moving in viscous fluid.

($F_{PA}$) acting on the aggregate particles by cement paste. Because of this normal stress, a friction force is developed between the aggregate particles and cement paste, which contributes to the mortar shear stress ($\tau_{FA-P}$). Based on Franzini and Finnemore, this normal force applied by the moving aggregate particles to the cement paste can be calculated according to Eq. (19) [14]. Thus,

$$F_{AP} = C_D \rho_P \frac{V_F^2}{2} A \tag{19}$$

where

$F_{AP}$ is force acting on cement paste by a moving aggregate particle;
$C_D$ is coefficient of the cement paste dragging force;
$\rho_p$ is cement paste density;
$V_F$ is particle fluctuation velocity; and
$A$ is projected area of a sphere aggregate particle, defined as $\pi D^2/4$, where $D$ is the average diameter of the particle.

The total normal stress applied to cement paste due to aggregate movement in a unit mortar, $\tau_{P-FA}$, is equal to the normal force generated by a single particle ($F_{AP}$) multiplied by the number of particles that move out of their host plane ($N_{collision}$), or the number of collisions in the flowing mortar, as given by Eq. (13):

$$\tau_{FA-P} = (k_P \cdot F_{AP}) \cdot N_{collision} \tag{20}$$

where

$\tau_{FA-P}$ is sub-total normal force acting on paste by aggregate particles in a horizontal plane;
$k_p$ is normal stress coefficient;
$F_{AP}$ is force acting on cement paste by a single aggregate particle; and
$N_{collision}$ is number of particles that move out of its host plane onto another adjacent plane (see Eq. (11)).

Here, the normal stress coefficient, $k_p$, is a term similar to the friction coefficient. It indicates that the shear force acted by the normal force of an aggregate particle ($F_{AP}$) on the surrounding cement paste increases with the magnitude of the normal force. $k_p$ is related not only to the material properties but also to the rate of the load applied to the mortar material [15].

### 3.5. Shear stress resulting from aggregate particle movements/collisions, $\tau_{FA}$

#### 3.5.1. Momentum change $(\Delta P_X)_0$ and energy loss $(\zeta)_0$ due to a two-particle collision

Fig. 10 illustrates a velocity diagram of a moving aggregate particle in a modeled mortar unit. Although randomly orientated, the aggregate moving velocity, $V$, can be expressed as

$$V = v_i + v_j + v_k \tag{21}$$

where $v_i$, $v_j$, and $v_k$ are velocity components along $X$, $Y$, and $Z$ axis, respectively.

The $X$ component of the particle velocity, $v_i$, can be further divided into two parts: $v_{i1}$ and $v_{i2}$. Assuming that one part of the velocity, $v_{i1}$, is equal to the overall mean flow velocity of mortar, $v_M$, $v_i$ can be expressed as

$$v_i = v_{i1} + v_{i2} = v_M + v_{i2} \tag{22}$$

Let $v_{i2}$ be considered together with $v_j$ and $v_k$ and determine

$$v_F = v_{i2} + v_j + v_k \tag{23}$$

where $v_F$ is called the fluctuation velocity of flowing particles. Thus, Eq. (20) becomes

$$v = v_M + v_F \tag{24}$$

The following section, therefore, determines the $v_M$ and $v_F$. Physically, the mean flow velocity, $v_M$, is generated by the drag force that the cement paste applies to a moving aggregate particle, which is in the mean flow direction. The fluctuation velocity, $v_F$, is generated by the collision of particles, which is randomly oriented. In the present study, all aggregate particles in the modeled mortar unit are assumed to have the same fluctuation velocity.

To analyze the mean flow velocity of colliding particles, a two-particle collision is first considered. As illustrated in Fig. 11, the relative positions of two colliding particles $A$ and $B$, both having the same mass and diameter but different moving velocities, are determined by angles $\Phi$ and $\Psi$. Based on the collision mechanics, the magnitude of the mean flow velocity between the two colliding particles $A$ and $B$ in the collision direction is [9,15,16] is:

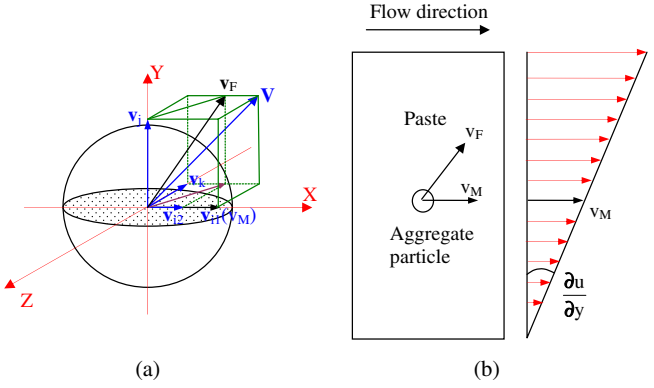


Fig. 10. Velocity components of a flowing particle.

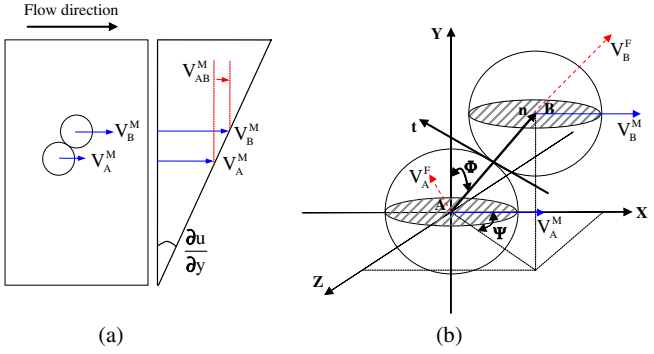


(a) (b)

Fig. 11. Illustration of collision between two particles.

$$V_{\mathrm{M}}^{n} = V_{AB}^{M} \cdot \sin\Phi \cdot \cos\Psi = D \cdot \frac{\partial u}{\partial y} \cdot \cos\Phi \cdot \sin\Phi \cdot \cos\Psi \tag{25}$$

where

$V_{AB}^{M}$ is relative mean flow velocity between particle A and B (Fig. 11);
$D$ is average diameter of aggregate particles; and
$\frac{\partial u}{\partial y}$ is velocity gradient of mortar.

The probability of a collision at a point on the surface of one sphere for this mean flow velocity is [17]:

$$P_{\mathrm{C}}^{M}(\Phi,\Psi) = \frac{\sin\Phi \cdot \mathrm{d}\Psi \cdot \mathrm{d}\Phi}{\pi} \tag{26}$$

where the range of $\Phi$ and $\Psi$ are $\Phi \in \left[-\frac{\pi}{2}, \frac{\pi}{2}\right]$ and $\Psi \in \left[0, \frac{\pi}{2}\right]$, respectively.

From Eqs. (24) and (25), the average mean flow velocity between the two colliding particles in the collision direction is

$$(V_{\mathrm{M}}^{n})_{\mathrm{AVE}} = \int\int_{\Phi,\Psi} V_{\mathrm{M}}^{n} \cdot P_{\mathrm{C}}^{M}(\Phi,\Psi) = 0.2122 \cdot D \cdot \frac{\partial u}{\partial y} \tag{27}$$

where

$D$ is average diameter of aggregate particles; and
$\frac{\partial u}{\partial y}$ is velocity gradient of mortar (shear strain rate).

Using a similar procedure (see Eqs. (21)–(26)), the average fluctuation velocity of particles $A$ and $B$ in the collision direction can be expressed as

$$(V_{\mathrm{F}}^{n})_{\mathrm{AVE}} = 0.6365 V_{\mathrm{F}} \tag{28}$$

where $V_{\mathrm{F}}$ is the magnitude of average fluctuation velocity of aggregate particles.

As shown in Fig. 11, the mean flow and fluctuation velocities between two colliding particles along the direction perpendicular to collision, $t$, are:

$$(V_{\mathrm{M}}^{t})_{\mathrm{AVE}} = 0.4244 \cdot D \cdot \frac{\partial u}{\partial y} \tag{29}$$

and $$(V_{\mathrm{F}}^{t})_{\mathrm{AVE}} = 0 \tag{30}$$

where $D$ and $\frac{\partial u}{\partial y}$ are the same as that in Eq. (24).

Based on continuum mechanics, the average momentum change, $(\Delta P_X)_0$, along the mean flow direction ($X$ direction in Figs. 10 and 11) and the kinetic energy loss, $\Delta E(=\zeta)$, due to collision of the two spheres are derived as [18]:

$$(\Delta P_X)_0 = \mu \cdot m \cdot (1+\varepsilon) \cdot \left(0.083 \cdot D \cdot \frac{\partial u}{\partial y} + 0.25 \cdot V_{\mathrm{F}}\right) \tag{31}$$

$$\Delta E = \frac{m}{4} \cdot (1-\varepsilon^2) \cdot \left\{\left[0.2122 \cdot D \cdot \frac{\partial u}{\partial y}\right]^2 + [0.6365 V_{\mathrm{F}}]^2\right\} + \frac{m}{4} \cdot \left\{\left(0.4244 \cdot D \cdot \frac{\partial u}{\partial y}\right)^2 - \left(0.4244 \cdot D \cdot \frac{\partial u}{\partial y} - \mu \cdot \left[0.2122 \cdot D \cdot \frac{\partial u}{\partial y} \cdot (1+\varepsilon) + 0.6365 V_{\mathrm{F}} \cdot (1+\varepsilon)\right]\right)^2\right\} \tag{32}$$

where

$(\Delta P_n)_0$ average momentum change of the two-particle collision in the collision direction,
$\Delta E$ energy loss due to the two-particle collision,
$D$ average diameter of aggregate particles,
$m$ average mass of aggregate particles,
$\frac{\partial u}{\partial y}$ velocity gradient of mortar,
$V_{\mathrm{F}}$ average fluctuation velocity of aggregate particles; it is the sum of $(V_{\mathrm{F}}^{\mathrm{n}})_{\mathrm{AVE}}$ and $(V_{\mathrm{F}}^{\mathrm{t}})_{\mathrm{AVE}}$, which are given in Eqs. (26) and (28),
$\mu$ friction coefficient of particles, and
$\varepsilon$ coefficient of elastic restitution.

### 3.5.2. Shear stress resulting from all aggregate particle movements or multiple-particle collisions, $\tau_{FA}$

As mentioned previously, the stress produced from the aggregate particle movements can be determined from the fundamental laws of continuum mechanics, Eqs. (2) and (3) [18]. The momentum change $\Delta P_X$ of two colliding spheres in the mean flow direction ($X$ direction), has been given by Eq. (31). The whole momentum change on a horizontal plane can be calculated by multiplying this single two-particle collision momentum, $(\Delta P_X)_0$ with the total number of collision occurring on this plane, $N_{\mathrm{collision}}$, are given by Eq. (13). Since the horizontal plane considered here is a unit plane, the total force acting on this plane gives the stress instead of the force. Thus, Eq. (2) was revised to:

$$\tau_{\mathrm{FA}} = N_{\mathrm{collision}} \cdot (\Delta P_X)_0 \tag{33}$$

where $\tau_{\mathrm{FA}}$ is the shear stress generated from the collision of aggregate particles in a horizontal plane.

Similar to momentum change, the total energy loss due to particle collisions of a unit horizontal plane can be determined by multiplying the energy loss of a single two-sphere collision system by the number of collisions:

$$\Delta E_{\text{collision}} = N_{\text{collision}} \cdot \Delta E \tag{34}$$

Energy loss due to interaction between one aggregate particle and the cement paste as it moves can be calculated according to the basic definition of energy:

$$\Delta E_{\text{interaction}}^{\text{single particle}} = F_{\text{AP}} \cdot S \tag{35}$$

where $F_{\text{AP}}$ is the force acting on cement paste by aggregate as given in Eq. (19), and $S$ is the average distance between the aggregate particles in mortar as given in Eq. (18).

Note that Eq. (35) provides calculation of the energy loss due to a two-spherical particle collision system. The total energy loss occurring in a unit horizontal plane can be determined as

$$\begin{aligned} E_{\text{interaction}} &= N_{\text{collision}} \cdot E_{\text{interaction}}^{\text{single particle}} \\ &= N_{\text{collision}} \cdot C_{\text{D}} \rho_{\text{P}} \frac{V_{\text{F}}^2}{2} A \cdot S \end{aligned} \tag{36}$$

where $N_{\text{collision}}$ is the effective number of collisions given by Eq. (13) and $C_{\text{D}}$ is the overall coefficient of drag.

Now, inserting Eq. (33) into Eq. (32) and plugging Eqs. (35)–(37) into Eq. (34), one can establish mortar shear stress by giving the energy dissipation due to aggregate particle collision ($\zeta$) equal to the total energy loss due to the aggregate particle collision and interaction with cement paste ($E_{\text{agg}}$):

$$\begin{aligned} N_{\text{collision}} \cdot (\Delta P_X)_0 \cdot \frac{\partial u}{\partial y} &= N_{\text{collision}} \cdot C_{\text{D}} \rho_{\text{P}} \frac{V_{\text{F}}^2}{2} A \cdot S \\ &\quad + N_{\text{collision}} \cdot \Delta E \end{aligned} \tag{37}$$

From Eq. (37), one can obtain the fluctuation velocity of aggregate particles, $V_{\text{F}}$ . Using Eq. (33), the shear stress from aggregate particle movement due to collision and friction, $\tau_{\text{FA}}$, is then determined.

Finally, the mortar shear stress expressed in Eq. (1) can be re-written as follows:

$$\begin{aligned} \tau_{\text{M}} = \tau_0 + \eta_{\text{P}} \cdot \frac{1 + 1.65 V_{\text{A}}}{1 - 1.35 V_{\text{A}}} \cdot \dot{\gamma}_m + k_{\text{P}} \cdot N_{\text{collision}} \cdot C_{\text{D}} \cdot \rho_{\text{P}} \\ \cdot \frac{V_{\text{F}}^2}{2} \cdot A + \tau_{\text{FA}} \end{aligned} \tag{38}$$

The viscosity of mortar can be obtained based on its rheological definition:

$$\eta_{\text{M}} = \frac{\tau_{\text{M}}}{\dot{\gamma} b} \tag{39}$$

where

$\eta_{\text{M}}$ mortar viscosity,
$\tau_{\text{M}}$ mortar shear stress, and
$\dot{\gamma}_{\text{M}}$ mortar shear rate.

The required inputs for use of the present model (Eq. (38)) are

- average diameter of the aggregate particles in the mortar ($D$),
- material density of aggregate ($\rho$),
- volume fraction of the aggregate ($V_{\text{A}}$),
- friction coefficient of the aggregate ($\mu$),
- coefficient of elastic restitution ($\varepsilon$),
- density, yield stress, and viscosity of cement paste ($\rho_{\text{p}}$, $\tau_{\text{p}}$, $\eta_{\text{p}}$, respectively), and
- overall coefficient of drag of cement paste ($C_{\text{D}}$).

## 4. Model application and verification

The present paper contains two subjects: (1) the mortar rheology model development and (2) application of the developed model for predicting mortar rheological behavior. The following sections focus on the second subject. In order to evaluate the validity of the new model, the general form of the newly developed particle–fluid model is derived, and the predicted results are discussed in a comparison with the existing (published) experimental research results.

### 4.1. General form of the particle–fluid model

If all parameters in Eq. (38) are collected from mortar mix design or computed based on the equations presented in this paper, Eq. (38) can be written as following:

$$\tau_{\text{M}} = \tau_0 + A \cdot \dot{\gamma} + B \cdot \dot{\gamma}^2 + C \cdot \dot{\gamma}^3 \tag{40}$$

where $A$, $B$, and $C$ are constant factors related to the mortar material properties, and which can be calculated from the equations provided in the previous section of this paper. The yield value $\tau_0$ is a real yield value, and $\dot{\gamma}$ is the shear rate. Eq. (40) shows that the new particle–fluid model has a power format, which is similar to both the modified Bingham model and the HB model [19]. Feys and colleagues have also verified a similar model to Eq. (40) based on experimental data from SCC rheology tests [20]. These instances prove that the present model is rational in physical interpretation and can be compared with the commonly used models.

### 4.2. Prediction of mortar rheological behavior

#### 4.2.1. Effect of cement paste properties

The basic cement properties used in the present model are yield stress and viscosity. These two basic rheological parameters are predominated by the cement properties, water-to-cement ratio (w/c), and the mixing method of the paste. To study the effect of cement paste properties on the rheological behavior of a mortar, two different cement pastes ($\tau_0 = 8$ Pa, $\eta = 0.12$ Pa s and $\tau_0 = 16$ Pa, $\eta = 0.24$ Pa s), one aggregate size (#16), and one volume content of aggregate (40%) are used in the newly developed particle–fluid model.

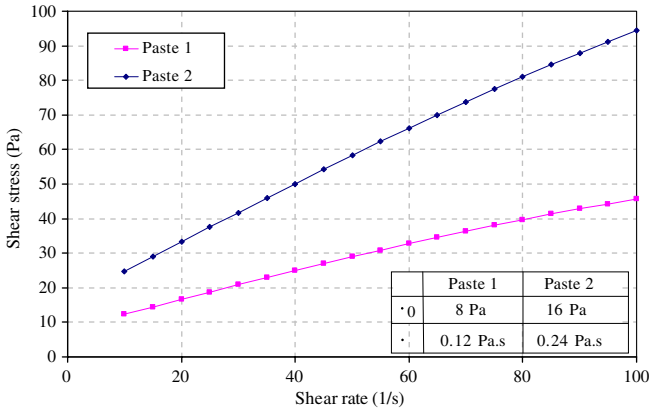


Fig. 12. Effect of paste properties on mortar rheological behavior (aggregate size #16 and volume 40%).

Fig. 12 shows the flow curves computed from the present model of the mortars made with different cement properties. As observed in the figure, both yield stress and viscosity of the mortars increase when the yield stress and viscosity of cement paste increase or w/c of the cement paste decreases. This indicates that a larger force is required to initiate the mortar flow and to maintain a high flow rate, which is consistent with the published results from mortar rheology testing and modeling [19–21].

*4.2.2. Effect of aggregate type*

The effect of aggregate properties on mortar rheology can be appropriately studied under the present model because an important aggregate property parameter, the coefficient of aggregate friction ($\mu$), is required as an input. The coefficient of aggregate friction ($\mu$) is associated with not only aggregate size and gradation but also the aggregate angularity and surface texture. Based on the results from a direct shear test and a mathematical model, the authors of the paper have obtained the coefficients of friction for various aggregates [22]. Using these friction coefficient values (0.5 for limestone and 0.3 for gravel), the shear stresses of mortars made with a cement paste ($\tau_0 = 16$ Pa, $\eta = 0.24$ Pa s) and two different types of aggregates (limestone and gravel), with a single size of #16, or 1.18 mm, and volume fraction of 40% are calculated according to the present particle–fluid model.

As observed in Fig. 13, for a given mix proportion and a given size of aggregate, limestone, having a higher coefficient of surface friction, provides the mortar with higher shear stress and viscosity than gravel.

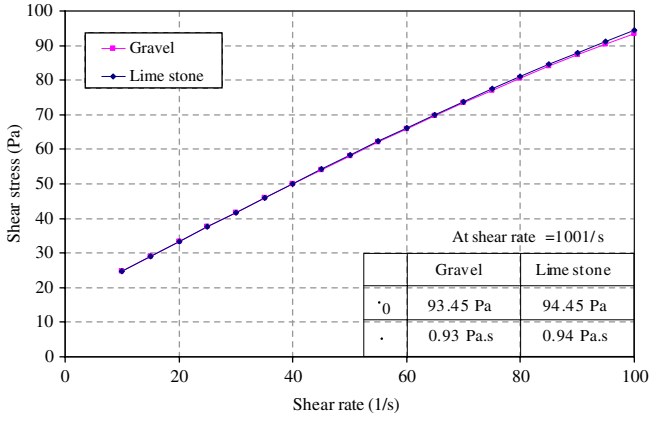


Fig. 13. Effect of aggregate type on mortar rheological behavior (aggregate size #16 and volume 40%; paste: $\tau_0 = 16$ Pa, $\eta = 0.24$ Pa s).

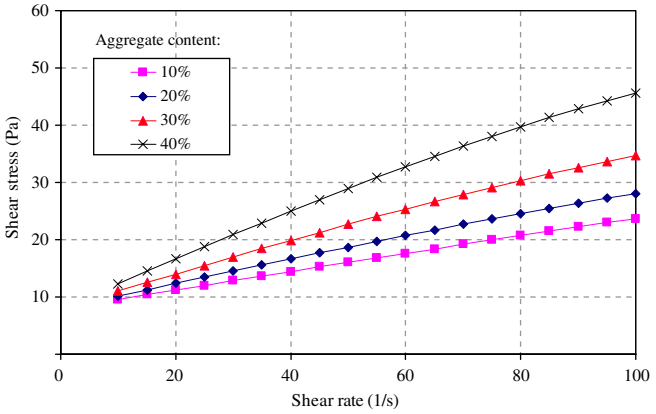


(a) Aggregate size: #16

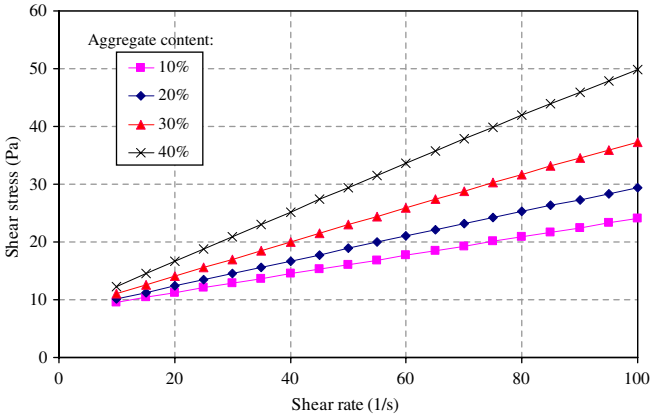


(b) Aggregate size: #30

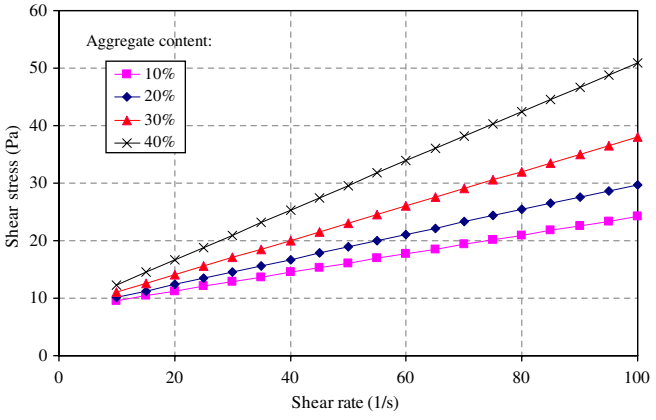


(c) Aggregate size: #50

Fig. 14. Effect of aggregate content on mortar rheological behavior (paste: $\tau_0 = 8$ Pa, $\eta = 0.12$ Pa s).

*4.2.3. Effect of aggregate content*

To investigate the effect of aggregate content on mortar rheology, one cement paste ($\tau_0 = 8$ Pa, $\eta = 0.12$ Pa s), three aggregate sizes (#16 or 1.18 mm, #30 or 0.6 mm, and #50 or 0.3 mm), and four volume fractions of aggregate (10%, 20%, 30%, and 40%) are considered. As shown in Fig. 14, the flow curves of mortars with different aggregate contents are significantly different. When the aggregate content increased, both the yield stress and viscosity of the mortar increase. This may be caused by the higher degree of friction and collision of solid particles, which increases the mortar shear stress and viscosity. Fig. 15 also shows that when the aggregate volume fraction increased from 10% to 40%, the mortar flow curves become increasing nonlinear. For a given volume fraction, larger aggregate sizes produced a more nonlinear flow curve compared to a smaller aggregate. This is mainly because that the collision of aggregate particles affects the flow of mortar more for larger aggregate particles than for smaller aggregate particles.

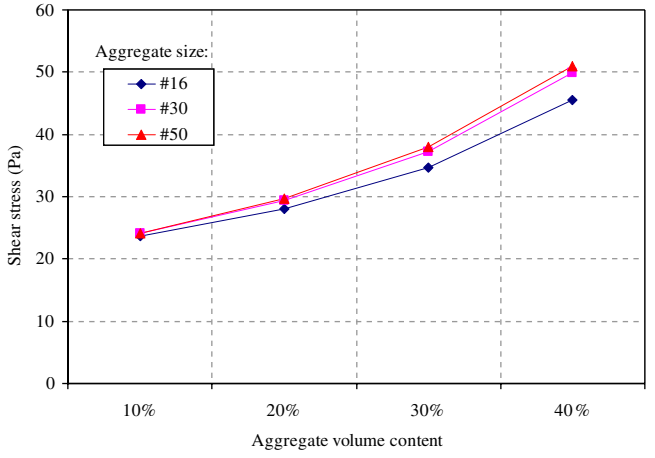


(a) Effect on shear stress

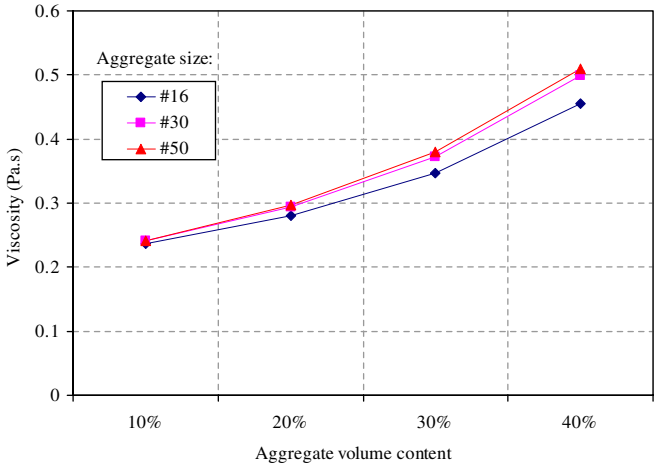


(b) Effect on viscosity

Fig. 15. Effect of aggregate content on mortar rheological parameters at shear rate=100 $s^{-1}$ (paste: $\tau_0 = 8$ Pa, $\eta = 0.12$ Pa s).

The effects of aggregate content on the mortar shear stresses and viscosities at shear rate of 100 $s^{-1}$ are summarized in Fig. 15. It is observed in the figure that at a low aggregate volume fraction (10% and 20%), the differences in the mortar rheological parameters (shear stress and viscosity) resulting from different sizes of aggregate are not significant. However, the differences become obvious when the volume fraction increases (30% and 40%).

*4.2.4. Studying the effect of aggregate size*

Fig. 14 also shows the effect of different aggregate sizes on mortar flow curves. For a given paste, aggregate material properties and volume fraction of aggregate, the mortar made with larger aggregate has a higher flowability. Again, at a low aggregate volume fraction (10% and 20%), the differences in the mortar rheological parameters (shear stress and viscosity) resulting from different sizes of aggregate are not significant (Fig. 15). However, the differences become obvious when the volume fraction increases (30% and 40%). The smaller aggregate size results in higher yield stress and viscosity of its mortar. This agrees with the common finding that a decrease in maximum size of aggregate generally increases the water demand of the concrete [23].

In summary, the results obtained from the present particle–fluid model have shown that the cement paste having higher flowability generally provides its mortar with lower viscosity and shear stress. In addition to the properties of the cement paste, aggregate size, gradation, and volume fraction significantly influence mortar rheology, among which the particle size distribution and aggregate gradation are of the most important significance. The present study on the effects of different aggregate types also demonstrates that the surface texture of aggregate has significant effect on the mortar rheology. The flowability of the mortar decreases with its aggregate volume fraction. For the mortar with a low aggregate volume fraction, the effect of aggregate size, gradation and surface texture on the mortar rheology is not significant, but this effect becomes significant as the volume fraction of aggregate increases. All these findings are consistent with the experimental results from mortar rheology tests [20,21].

## 5. Concluding remarks

A particle–fluid model was developed for studying the flow behavior of highly flowable mortar. In this model, fresh mortar is considered as a two-phase material, with a fluid matrix and a group of rigid particles dispersing in the matrix. The mortar shear stress is considered as the sum of shear stresses resulting from the cement paste flow and the aggregate particle movements as well as the interaction between the cement paste and aggregate. The new model shows a power function between the shear stress and shear of a mortar, which agrees with the widely-accepted "modified Bingham" model and Herschel–Bulkley (HB) model. Different from these commonly-accepted

models, the new particle–fluid model itself illustrates the factors that affect mortar behavior (such as cement paste density and rheological properties as well as aggregate characteristics and volume fraction). Using this new model, the effects of these factors were investigated, and the results obtained from the new model are consistent with those from the published experimental tests.

## Acknowledgement

The present work is a part of the first author's Ph.D. dissertation. The author would like to acknowledge the National Concrete Pavement Technology Center (CP Tech Center) for support of his study at Iowa State University.

## References

[1] Okamura H, Ouchi M. Self-compacting concrete. J Adv Concr Technol 2003;1(1):5–15.
[2] Larrard D, Ferraris CF, Sedan T. Fresh concrete: a Herschel–Bulkley material. Mater Struct 1998;31(211):494–8.
[3] Bird RB, Dai GC, Yarusso BJ. The rheology and flow of viscoplastic materials. Rev Chem Eng 1983;1:1–70.
[4] Topcu IB, Kocataskin F. A two-phase composite materials approach to the workability of concrete. Cement Concr Compos 1995;17(4):319–25.
[5] Kurokawa Y, Tanigawa Y, Mori H, Nishinosono K. Analytical study on effect of volume fraction of coarse aggregate on Bingham's constants of fresh concrete. Trans Jpn Concr Inst 1996;18:37–44.
[6] Pimanmas A, Ozawa K. Mathematical modeling of shear constitutive relationship for flowing fresh concrete. In: Proceedings of ICU-EACC, Bangkok, Thailand, 1996; p. D.128–D.133.
[7] Kennedy CT. The design of concrete mixes. Proc Amer Concr Inst 1940;36:373–400.
[8] Su N, Hsu K, Chai H. A simple mix design method for self-compacting concrete. Cem Concr Res 2001;31(12):1799–807.
[9] Oh SG, Noguchi T, Tomosawa F. Toward mix design for rheology of self-compacting concrete. In: RILEM international symposium on self-compacting concrete, University of Tokyo; 1999.
[10] Nehdi M, Mindess S. Applicability and significance of rheometric tests for rheology of fluid and self-leveling high-strength concrete. Transport Res Rec 1996;1574:41–8.
[11] Harr ME. Mechanics of particulate media—a probabilistic approach. New York: McGraw-Hill; 1977.
[12] ASTM C33-03, Standard specification for concrete aggregates, Annual Book of ASTM Standards, vol. 04. 02; 2003.
[13] Cadle RD. Particle size; theory and industrial applications. New York: Reinhold Publishing Corporation; 1965.
[14] Franzini JB, Finnemore EJ. Fluid mechanics with engineering application. New York: McGraw-Hill; 1997.
[15] Duran J. Sands, powders, and grains—an introduction to the physics of granular materials. New York: Springer-Verlag; 1999.
[16] Goldsmith W. Impact the theory and physical behaviour of colliding solids. London: Edward Arnold; 1960.
[17] Mehrabadi MM, Nemat-Nasser S, Oda M. On statistical description of stress and fabric in granular Mechanics. Int J Numer Anal Methods Geomech 1982;6(1):95–108.
[18] Fung YC. Continuum mechanics. New Jersey: The Prentice-Hall; 1977.
[19] Ferraris CF. Measurement of the rheological properties of high performance concrete: state of the art report. J Res Natl Inst Stand Technol 1999;104(5):461–77.
[20] Feys D, Verhoeven R, DeSchutter G. Fundamental study of the rheology of Self Compacting Concrete, composed with Belgian materials. In: The 7th national congress on theoretical and applied mechanics NCTAM; 2006.
[21] Hu J. A study of effects of aggregate on concrete rheology. PhD thesis. Ames, Iowa State University; 2005.
[22] Lu G, Wang K. Predicting friction of granular materials using a 3-D probabilistic model approach, submitted for publication.
[23] Mehta PK, Monteiro PJM. Concrete-structure, properties and materials. 2nd ed. Prentice-Hall; 1993.